https://doi.org/10.31436/iiumej.v24i1.2604

CONTROL STRATEGY FOR POWER ASSIST UPPER LIMB REHABILITATION ROBOT WITH THE THERAPIST'S MOTION INTENTION PREDICTION

ZULIKHA AYOMIKUN ADEOLA-BELLO[1], NORSINNIRA ZAINUL AZLAN[1*] AND SALMAH ANIM ABU HASSAN[2]

[1]Department of Mechatronics Engineering, Kulliyyah of Engineering, International Islamic University Malaysia, Jalan Gombak, 53100 Kuala Lumpur, Malaysia
[2]Department of Orthopaedics, Traumatology and Rehabilitation, Kulliyyah of Medicine, International Islamic University Malaysia Kuantan Campus, Jalan Sultan Ahmad Shah, Bandar Indera Mahkota, 25200 Kuantan, Pahang, Malaysia

**Corresponding author: sinnira@iium.edu.my*

(Received: 15th September 2022; Accepted: 1st December 2022; Published on-line: 4th January 2023)

ABSTRACT: Currently, fully automated rehabilitation robots can assist therapists in providing rehabilitation therapy, hence the patients could get hurt. On the other hand, manual treatment may cause less patient injury but it is tiresome, and there are not enough therapists in most countries. Power assist rehabilitation robots can support the therapists in conducting the treatment and may help to alleviate this problem. The goal of this study is to develop a control strategy for the robot to assist the therapist's movement in a power assist upper limb rehabilitation treatment. The system combines the advantages of robotic and manual rehabilitation therapy. Torque and position sensors fitted on the power assist upper limb rehabilitation robot arm are used for motion intention estimation. The amount of angular velocity necessary to be delivered to the feedback controller will be determined by predicting the therapist's motion intention using the impedance control method. The resulting velocity from the motion intention estimator is incorporated into the Sliding Mode Control - Function Approximation Technique (SMC-FAT) based adaptive controller. The SMC-FAT based adaptive controller in the feedback loop, overcomes the uncertain parameters in the combination of the robot and the human arm. The motion intention estimator forecasts the movement of therapists. The proposed controller is used to regulate elbow flexion and extension motion on a power assist upper limb rehabilitation robot with one degree of freedom (DOF). The proposed control system has been tested using MATLAB simulation and hardware experimental tests. The outcomes demonstrate the effectiveness of the proposed controller in directing the rehabilitation robot to follow the desired trajectory based on the therapist's motion intention, with maximum errors of 0.002rad/sec, 0.005rad/sec and 0.02rad/sec for sinusoidal, constant torque values, and hardware experiment respectively.

ABSTRAK: Pada masa ini, robot rehabilitasi automatik sepenuhnya dapat membantu ahli terapi dalam menyediakan terapi pemulihan, tetapi pesakit berkemungkinan tercedera. Sebaliknya, rawatan manual berkemungkinan mengurangkan kecederaan pesakit tetapi ia memenatkan, dan terdapat kurang ahli terapi yang mencukupi di kebanyakan negara. Robot pembantu rehabilitasi dapat membantu ahli terapi dalam menjalankan pemulihan dan mengurangkan masalah ini. Sistem ini menggabungkan kelebihan terapi pemulihan robotik dan manual. Alat pengesan tork dan kedudukan diletakkan pada anggota atas lengan robot rahabilitasi yang digunakan bagi mengesan anggaran jarak pergerakan ahli terapi. Anggaran halaju sudut diperlukan bagi kawalan gerak balas dan dapat diketahui melalui anggaran niat gerakan ahli terapi menggunakan kaedah kawalan impedans. Halaju yang terhasil daripada anggaran niat gerakan diadaptasi ke dalam pengawal adaptif berasaskan Kawalan Mod

Gelongsor - Teknik Anggaran Fungsi (SMC-FAT). Pengawal penyesuaian berasaskan SMC-FAT dalam gelung maklum balas, mengatasi parameter yang tidak pasti dalam gabungan robot dan lengan manusia. Penganggar niat gerakan meramalkan gerakan ahli terapi. Pengawal yang dicadangkan digunakan bagi mengawal lenturan siku dan gerakan lanjutan pada robot rehabilitasi dengan satu darjah kebebasan (DOF). Sistem kawalan yang dicadangkan telah diuji menggunakan simulasi MATLAB dan ujian eksperimen perkakasan. Dapatan kajian menunjukkan keberkesanan pengawal yang dicadangkan dalam mengarahkan robot rehabilitasi mengikut trajektori yang dikehendaki berdasarkan niat gerakan ahli terapi, dengan ralat maksimum masing-masing 0.002rad/s dan 0.005rad/s bagi sinusoidal, nilai tork malar, dan eksperimen perkakasan masing-masing.

KEYWORDS: *Upper Limb rehabilitation; Motion intention estimator; uncertainties; therapist assistance; rehabilitation robot*

1. INTRODUCTION

Stroke victims frequently lose their ability to do daily tasks with their hands. Stroke is regarded as one of the most serious diseases and a vital issue in the nation because of the large number of its victims. Patients can restore arm functions and resume doing routine and essential daily tasks after intensive practice that is repeated and massed over the rehabilitation process. The two categories of power assist upper limb rehabilitation robots are end-effector and exoskeleton robots. These robots can conduct a variety of actions and undertake rehabilitation training activities to help patients complete certain therapies [1]. Additionally, it offers a consistent and demanding physical treatment, relieving physical therapists of a substantial amount of labor. End-effector systems may move limbs in space without requiring the patient's and robot's joints to be aligned by using footplates or grips.

Manual rehabilitation therapy and robotic rehabilitation therapy are two rehabilitation approaches. A global issue with manual rehabilitation treatment is its inconsistency and its low therapist-to-patient ratio. The entirely autonomous nature of earlier rehabilitative equipment increases the potential for patient injury. This issue can be solved by a rehabilitation robot that combines manual and automated functions. The study focuses on a new control approach for a power assist rehabilitation robot that aids the therapist in moving the patient's arm during rehabilitation exercises, allowing the system to combine the advantages of completely robotic and manual rehabilitation treatment. In this manner, the system may provide patients with a rehabilitation program that is both safe and comfortable [2].

This paper presents a new control approach for the therapist, allowing them to actively intervene in the treatment, taking into account the robot and patient's parameter uncertainties. The controller consists of a motion intention estimator for the therapist based on the impedance controller. The resulting output velocity is fed into the FAT-SMC based adaptive controller to cater to the uncertainties. The novelty of this paper is a new control strategy that focuses on assisting the therapist's movement with a motion intention estimator combined with SMC-FAT based adaptive controller in the feedback loop for a power assist upper limb rehabilitation robot.

The rest of the paper is organized as follows. Section 2 presents the summary of previous works on upper limb rehabilitation robot and motion intention estimation. Section 3 describes the methods and equations used in deriving the proposed control strategy. The simulation results and hardware experimental analysis are discussed in Section 4. Section 5 presents the conclusion of the paper.

https://doi.org/10.31436/iiumej.v24i1.2604

2. PREVIOUS WORKS ON UPPER LIMB REHABILITATION ROBOT AND MOTION INTENTION ESTIMATION

Due to the lack of a direct therapist intervention during training, the use of totally robotic rehabilitation treatment may increase the risk of patients' injuries and may be uncomfortable for the patients [3]. Additionally, mistakes in the treatment robot's actuation are possible. Thus, this paper presents a new control strategy for the upper limb rehabilitation robot that is not fully robotic and assists the therapist based on their motion intention to realize a smooth movement in the rehabilitation. This section represents the previous work in power assist upper limb rehabilitation robot and motion intention estimation methods.

2.1. Power Assist Upper Limb Rehabilitation Robot

Power assist devices are created and intended to help physically challenged persons with everyday chores and self-rehabilitation. Tang et al. [4] developed an upper-limb power-assist exoskeleton actuated by pneumatic muscles. The exoskeleton may now be controlled in real time depending on the user's intended movements thanks to the development of proportional myoelectric control. The feature extraction technique and classification were utilized to create an electromyogram (EMG)-angle model for pattern recognition.

An approach for perception-assist that modifies the user's mobility as necessary to help their movement and interaction with their environment was proposed [5]. A study on a power-assist robot arm using pneumatic artificial rubber muscles (PARMs) with a balloon sensor was published to help with upper-limb and back motions. The elbow and wrist joints may be moved by a single PARM, and the movement of the various arm portions is similar to that of the bi-articular muscle. According to the independent joint control paradigm, an ideal linear quadratic Gaussian torque controller (LQG) with integral action for an upper limb rehabilitation robot was introduced. The controller's goals are to simplify the control design process, guarantee the best robust torque control, and prevent modeling uncertainties.

2.2. Motion Intention Estimation Methods

The intended velocity, which serves as a proxy for human intention is determined in real-time using the robot's location, speed, and interaction force as well as contact point movement characteristics [6]. Impedance control, which enables the robot to follow a specified path, may be used for interaction control. The techniques for changing the assistance lever of the impedance parameters are often employed in various applications of human-robot shared control systems.

The Radial-based Function Neural Network (RBFNN) model for evaluating the cooperation intention in touch human-robot collaboration has been developed. Lee et al. [7] suggested a new classifier based on force information measured by the robot's Force/Torque sensor and surface EMG signals from muscle activation to extract human intention during interaction with external force. The degree of external force produced by the encounter may be determined using the suggested classifier. In order to validate the suggested methodology, a simple control method is developed based on the proposed classifier to support the intention-based motion.

A device that produce the intended trajectory based on the designer's assessment of the user's motion intention was introduced. Motion intention was proposed as a workable solution since it takes a lot of energy for a person to move the exoskeleton arm, especially if the difference between the robot's true position and the human's motion intention is large. The subject's desired intention of motion (DIM) must be determined via an indirect force control loop. The identification of DIM can be accomplished using the Damped Least Square technique (DLS).

A wearable double-shell robotic exoskeleton for upper-limb power assist was proposed by Huang et al. [8], based on an online assessment of the wearer's motion intention.

A unique method for identifying human body motion intention for active power-assist lower limb exoskeleton robots (APAL) was investigated [9]. Both the inverse dynamics approach (IDA), which uses a dynamic model of the human body, and the sensing system integrated within an exoskeleton robot (APAL), which was developed to gather motion data and foot contact force, were used to do online estimations of the human joint torque. An approach to evaluate interaction motion intention for perception-assist with an upper-limb wearable power-assist robot was given in a work by [10]. The power-assist wearable robot user was given instructions to use visual information from the camera that was worn to assess the other person's motion intention in this approach.

The problem of tracking the user's motion intentions when they were using an upper-limb power-assist wearable robot in planned social interactions with other people was addressed by [11]. If the interaction is inappropriate, the power-assist wearable robot's user motion can be automatically changed to guarantee excellent interaction performance or to prevent unforeseen mistakes when using the device.

Surface electromyography (SEMG), a bioelectrical signal created when a neuron conveys human motion intention information directly to a related muscle, is an example of artificial intelligence-based estimate. Therefore, without any information loss or delay, the motion's purpose may be fully inferred. Due to its wealth of data, superior collecting technology, and noninvasiveness, human motion intention recognition based on SEMG will become widely used. Machine learning (ML) based motion and SEMG-driven musculoskeletal (MS) model-based motion are the two methods of SEMG-based motion intention recognition. The most important aspect of the entire procedure is determining human motion intentions [12].

A neuro-fuzzy technique for accurately anticipating the motion intention of the power-assist rehabilitation robot user was proposed, taking the effect of the difference in posture into consideration. It seems that many sensor modalities are needed for sophisticated device control given the challenges of providing reliable control with simply EMG. An EMG-based admittance controller (EAC) was created to address the problem. Determining the human purpose for a multifunctional device's successful use and effective operation presents a number of challenges, though. The primary rationale is the time-varying and noisy character of the EMG signals [13]. In addition, there is a complicated non-linear connection between the output forces of the various muscles.

Extreme Learning Machine (ELM), a revolutionary approach, was suggested as a solution to these problems [14]. Using radial basis function networks, single and multi-hidden layer neural networks, feed-forward neural networks may be generalized effectively. However, because these approaches are sluggish when simulating a broad class of natural occurrences, they are unsuitable for applications like discerning human purpose. The need to fine-tune each network parameter is the fundamental reason for this delayed learning. Based on information from force sensors, joint current location, and current moving speed, ELM can quickly assess desired goals, learn human motion patterns, and forecast future movement. In assistive robotics and rehabilitation, this desired motion may be used to increase performance and robot compliance. An exoskeleton-style rehabilitation or assistance robot may be managed more successfully and comfortably by the user by utilizing the recommended interface, intention estimate, and intention-based control algorithms [15]. The rehabilitation power-assisted robot must be able to increase its output proportionally to the amount of mobility required.

Utilizing EMG data, a lower limb neuromusculoskeletal model was used to determine the torque at each human joint before applying an admittance control strategy to attain the desired position. A synchronized and robust Human-Robot Interaction (HRI) was produced using an EMG-based admittance controller (EAC). Wang et al. [16] employed neural networks to discover model parameters online before adding the desired trajectory into the impedance control of an upper-limb humanoid robot. To illustrate the expected course of human mobility, they created a model of an upper human limb. When the human motion intention is unsure and the robot dynamics are unknown, an interactive robot utilizes adaptive impedance control. It was found that the joint torque of the human body fits the essential requirements of motion intention estimate for the active power-assist after looking at the conduction path and numerous stage manifestations of motion intention in the human body. Joint torque is also said to create real-time, continuous output, precede human limb movements, and indicate the intensity and direction of the wearer's efforts. This calls for the need for an accurate model, an evaluation of human intent, and a method for measuring human joint torque.

Conventional control systems based on force/torque sensors have difficulty interpreting human intentions and are typically susceptible to misreading or distorting such intentions because of external contact force interruptions, such as those experienced in daily activities. Therefore, a power-assist robot controller cannot accurately evaluate the real human force. Force/torque sensors are used to measure the overall amount of applied force, which includes both human intention and unidentified environmental factors. The power assist robot may also employ motion sensors on the user to facilitate the anticipated actions. For a power support exoskeleton robot arm, a motion intention-based bionic control system was suggested [17]. To pre-process the recorded motion signal, filtering is utilized.

An improved robot skill learning system that took motion production and trajectory tracking into account, was suggested by [18]. During robot learning demonstrations, dynamic movement primitives (DMPs) were used to imitate robotic mobility. Each DMP is composed of a number of dynamic systems that act in concert to increase the stability of the motion toward the aim. A hybrid force/position control approach for robotic arms based on the stiffness estimation of an unknowable environment was developed to provide precise control and a stable system. Predicting human intent necessitates human-robot interaction.

The primary aspect affecting the creation of upper limb rehabilitation robots is human motion intention. Since assistive or rehabilitative robots must move in line with the wearer's request, estimating the wearer's motion intention is a key challenge. For Power support systems for wearables, it is extremely important to design an effective identification method for identifying the wearer's motion intention. Thus, in this research, the impedance control interaction strategy is used for motion intention estimation of the therapist and SMC-FAT-adaptive controller is used to cater for the parameter uncertainties for a power assist upper limb rehabilitation robot with patient's arm.

3. PROPOSED CONTROL STRATEGY

The block diagram for the proposed control strategy is shown in Fig. 1. The motion intention controller calculates the therapists' motion prediction, and it is integrated into the SMC-FAT controller. This controller acts as the feedback controller to cater to the patient's arm parameter uncertainties [19]. It takes the information of the desired trajectory, x_d , actual angular velocity, $\dot{q}$, and therapist's torque, τ_h to calculate the desired velocity, $\dot{q_d}$, for the therapist's motion intention estimation. The value is then passed to the SMC-FAT controller. The outcome is integrated into the lumped rehabilitation robot and human arm plant.

https://doi.org/10.31436/iiumej.v24i1.2604

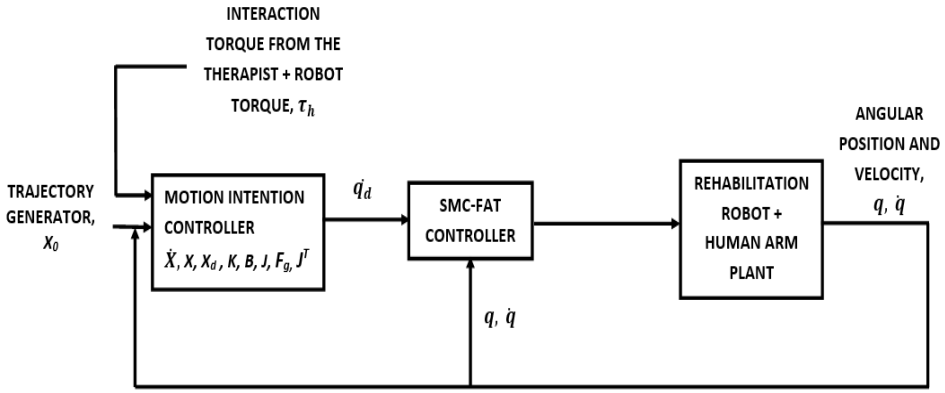

Fig. 1. Block diagram of control strategy

Fig. 2 shows the block diagram of the experimental setup. The angular position of the robot's joints with the patient's arm and therapist's torque exerted will be measured using encoders and torque sensors respectively, and supplied to the microcontroller. The amount of desired angular velocity based on the motion prediction of the therapist will be calculated. The necessary amount of voltage required for assisting the therapist will be provided to the upper limb rehabilitation robot from the SMC-FAT based adaptive controller.

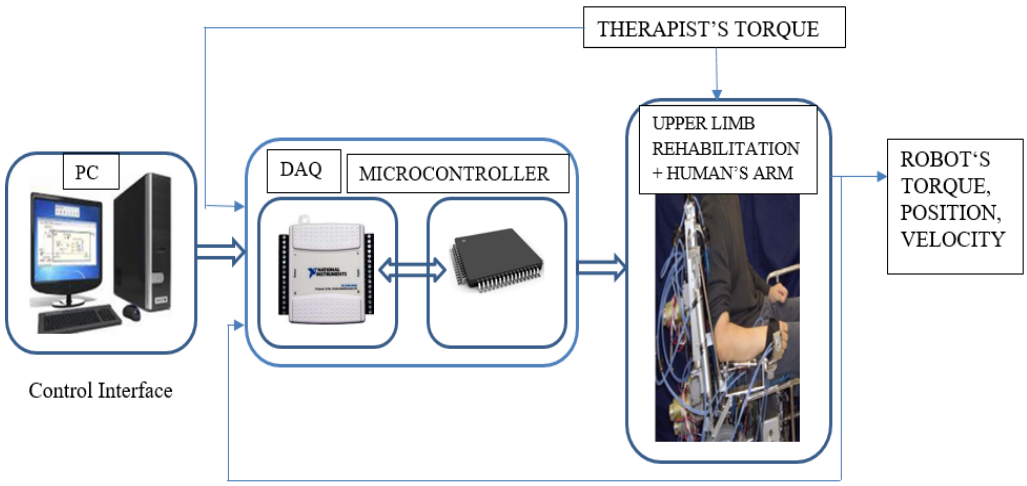

Fig. 2. Block diagram of the experimental architecture

In this research, torque and position sensor measurements are used to calculate the therapist's motion intention prediction. The therapist's torque exerted and the robot joint's angular position are the quantities that will be measured. The therapist's torque is calculated using constant torque and sinusoidal value. The robot torque and position trajectory of the robot can only be derived from the output of the lumped upper limb rehabilitation robot and human arm, after the implementation of motion intention estimator and SMC-FAT- adaptive controller. The DAQ helps to communicate between the computer (PC) and the robot. In this research, a serial communication DAQ (NI USB-6211) is used, and it is connected to the Upper limb rehabilitation robot. The role of the PC is to program the controller and also serve as interface to help tune and display the control parameters. The LabVIEW and the NI-DAQmx driver are installed into the PC to test the proposed controller on the power assist upper limb rehabilitation robot. Simulation and hardware experimental tests are used to evaluate the performance of the project with the aid of MATLAB and LabVIEW softwares.

https://doi.org/10.31436/iiumej.v24i1.2604

3.1. Dynamic Model of the Integrated Power Assist Upper Limb Rehabilitation Robot with Human Arm

The dynamic model of the upper limb rehabilitation robot with human arm can be written below. The mathematical model of the system is adopted from [20].

$$\dot{X}_B = A_B X_B(t) + B_B U_s(t) + F_B T(t) + W_B \dot{T}(t) \tag{1}$$

where, A_B, B_B, F_B, W_B are the system, input, load distribution, and rate of load distribution matrices with acceptable dimensions respectively. $X_B(t)$ is the vector consisting of the angular position, velocity, and acceleration of the electrical motor. $U_s(t)$ is an input vector, $T(t)$ is the mechanical link torque and $\dot{T}(t)$ is its time derivative.

where,

$$X_B(t) = [x_1 \quad x_2 \quad x_3] \tag{2}$$

$$= [x^1{}_B \quad x^2{}_B \quad x^3{}_B] \tag{3}$$

$$= [q \quad \dot{q} \quad \ddot{q}\,] \tag{4}$$

$$A_B = \begin{bmatrix} 0 & 1 & 0 \\ 0 & 0 & 1 \\ 0 & a_{B32} & a_{B33} \end{bmatrix} \qquad B_B = \begin{bmatrix} 0 \\ 0 \\ b_B \end{bmatrix} \qquad F_B = \begin{bmatrix} 0 \\ 0 \\ f_B \end{bmatrix}$$

$$W_B = \begin{bmatrix} 0 \\ 0 \\ w_B \end{bmatrix} \qquad U(t) = [U(t)] \qquad T(t) = [T(t)] \qquad \dot{T}(t) = [T(t)] \tag{5}$$

The non-zero elements of the A_B, B_B, F_B and W_B matrices are as follows [20]:

$$a_{B32} = -\frac{k_v k_t + B_v R}{J_m L} \qquad a_{B33} = -\frac{B_v L + J_m R}{J_m L}$$

$$b_B = \frac{k_t}{J_m L N}$$

$$f_B = -\frac{R_2}{N^2 J_m L} \qquad w_B = -\frac{1}{N^2 J_m} \tag{6}$$

where,

J_m is the moment of inertia, R is the armature resistance, L is the armature inductance, B_v is the viscous friction constant, k_v is the Back Emf constant, and N is the inverse of gear ratio [20].

The dynamic equation of the mechanical links of the 1 DOF rehabilitation robot with human arm can be written as follows.

$$T(t) = M(q(t), \zeta)\ddot{q}(t) + \bar{D}(q(t), \zeta)\hat{V}(\dot{q}) + G(q(t), \zeta) + F_c\, sgn(\dot{q})s + V_c\dot{q}(t) \tag{7}$$

https://doi.org/10.31436/iiumej.v24i1.2604

where,

$$q(t) = [q(t)]^T \tag{8}$$

$$T(t) = [T(t)]^T \tag{9}$$

$$M(q,\zeta) = [M] \tag{10}$$

$$\bar{D}(q,\zeta) = [\bar{D}_{11} \quad 0 \quad 0 \quad 0 \quad \bar{D}_{15} \quad \bar{D}_{16}]$$

$$\hat{V}(\dot{q}) = [\dot{q}], \qquad G(q) = [G] \tag{11}$$

$$Fc = [F_C] \qquad Vc = [V_C] \tag{12}$$

where,
q is the joint angular position
$\dot{q}$ is the joint angular velocity
$\ddot{q}$ is the joint angular acceleration
$M(q,\zeta)$ is the positive definite inertia matrix.
$\bar{D}(q,\zeta)$ is the Coriolis and Centrifugal torques.
$G(q,\zeta)$ is the gravitational torque.
$\zeta$is the uncertain human arm mass carried by the rehabilitation robot.
T is the control input torque from the actuators.
Fc and *Vc* are the coulomb friction coefficients and viscous friction coefficients respectively.
The terms $\bar{D}(q,\zeta)\,\hat{V}(\dot{q})$ and $G(q,\zeta)$ in Eq. (7) can be modified as $\hat{D}(q,\dot{q},\zeta)\,\dot{q}$ and $\hat{G}(q,\zeta)q$ respectively. Hence, the lumped 1DOF rehabilitation robot with human arm dynamic model can be rewritten as:

$$T(t) = M(q(t),\zeta)\ddot{q}(t) + \hat{D}(q(t),\dot{q}(t),\zeta)\dot{q}(t) + \hat{G}(q(t),\zeta)q(t) + F_c[sgn(\dot{q})q(t)] + V_c\dot{q}(t) \tag{13}$$

where,

$$\hat{D}(q,\dot{q},\zeta) = [D\dot{q}] \tag{14}$$

$$\hat{G}(q,\zeta) = \left[\frac{G}{q}\right] \quad \widehat{sgn}(\dot{q}) = \left[\frac{sgn(\dot{q})}{q}\right] \tag{15}$$

The derivative of the torque with respect to time for 1 DOF rehabilitation robot with human arm from Eq. (13) can be written as

$$\dot{T}(t) = M(q,\zeta)\dddot{q}(t) + \tilde{C}(q,\dot{q},\zeta)\ddot{q}(t) + \tilde{D}(q,\dot{q},\zeta)\dot{q}(t) + F_c[sgn(\dot{q})\dot{q}(t)] + F_c q\frac{d}{dt}(sgn(\dot{q})) + V_c\ddot{q}(t) \tag{16}$$

By substituting Eq. (13) and Eq. (16) into the augmented actuator dynamic Eq. (1), the integrated dynamic model of a 1-DOF rehabilitation robot with human arm can be obtained in the following form. Only one joint of rehabilitation robot is considered in this study, which is the elbow for flexion and extension. The robot and human arm are considered as lumped body. The dynamic model is taken from [20] and can be written as:

$$\dot{X}_B(t) = A_B(X_B,\zeta,t)X_B(t) + B_B(X_B,\zeta,t)U(t) \tag{17}$$

where,

$$A_B(X_B,\zeta,t) = [I_3N - W_BM(X_B,\zeta,t)Z_B]^{-1}\{A_B + [F_BM(X_B,\zeta,t) + W_B\tilde{C}(X_B,\zeta,t) + W_BV_C]Z_B + [F_B\hat{D}(X_B,\zeta,t) + F_BV_C(X_B,\zeta,t) + W_B\tilde{D}(X_B,\zeta,t) + W_BF_C\widehat{sgn}(\dot{q}) +$$

https://doi.org/10.31436/iiumej.v24i1.2604

$$W_B\hat{d}(t)]Z_{B1} + [F_B\hat{G}(X_B,\zeta,t) + F_BF_C\, sgn(\dot{q}) + F_B\hat{d}(t) + W_B\dot{\hat{d}}(t) + W_BF_C\left[\frac{d}{dt}((\dot{q}))\right]Z_{B2}\} \quad (18)$$

$$B_B(X_B,\zeta,t) = [I_3N - W_BM(X_B,\zeta,t)Z_B]^{-1}B_B \quad (19)$$

Then, the integrated model of the 1-DOF robot manipulator can be obtained and has the following form:

$$\grave{X}_B(t) = A(X_B,\zeta,t)X_B(t) + B(X_B,\zeta,t)U(t) \quad (20)$$

where,

$$A_B(X_B,\zeta,t) = \begin{bmatrix} 0 & 1 & 0 \\ 0 & 0 & 1 \\ a_{B31} & a_{B32} & a_{B33} \end{bmatrix} \quad (21)$$

$$B(X_B,\zeta,t) = [b] \quad (22)$$

A detailed explanation of the dynamic model of the rehabilitation robot exoskeleton with human arm can be found in [20] , which will serve as a guide for the derivation of the integrated model of the 1 DOF robot arm.

3.2. Motion Intention Controller

For the motion intention controller, the impedance control is adopted [21]. Impedance control is defined as the relationship between the motion state of the endpoint and applied force. The relationship between the therapist's torque, τ_h, contact force, F_{ext} and transpose form of the Jacobian vector of the exoskeleton is given as [22].

$$\tau_h = J^T F_{ext} \quad (23)$$

The target impedance adopted from [22] is given as a second-order differential equation and can be written as

$$M(\ddot{X} - \ddot{X}_d) + B(\dot{X} - \dot{X}_d) + K(X - X_d) = -F_{ext} \quad (24)$$

For this research, only one degree of freedom is used. To overcome some practical challenges in impedance control, F_g is the extra gravity compensated force is considered [23]. Eq. (24) is modified as.

$$M(\ddot{X} - \ddot{X}_d) + B(\dot{X} - \dot{X}_d) + K(X - X_d) = -F_{ext} - F_g \quad (25)$$

$M(\ddot{X} - \ddot{X}_d)$ is omitted for simplicity. Therefore, Eq. (25) can be written as.

$$B(\dot{X} - \dot{X}_d) + K(X - X_d) = -F_{ext} - F_g \quad (26)$$

where,
M is the moment of inertia
$\ddot{X}$ is the actual acceleration
$\ddot{X}_d$ is the desired acceleration
$\dot{X}$ is the actual velocity
$\dot{X}_d$ is the desired velocity
X is the actual position
X_{d} is the desired position
B is the damping coefficient
K is the stiffness
F_g is the extra gravity compensated force.

https://doi.org/10.31436/iiumej.v24i1.2604

A relationship between the target speed and the interaction torque of each joint is necessary to obtain the motion intention estimation [24]. Thus, the angular velocity needs to be converted to the velocity of the endpoint of the robotic arm by using the Jacobian matrix [24]. Hence, Eq. (26) is multiplied by the Jacobian matrix, J^T

$$J^T B\left(\dot{X} - \dot{X}_d\right) + J^T K(X - X_d) = -J^T F_{ext} - J^T F_g \tag{27}$$

Substituting Eq. (23). into Eq. (27) yields.

$$J^T B\left(\dot{X} - \dot{X}_d\right) + J^T K(X - X_d) = -\tau_h - J^T F_g \tag{28}$$

Expand and simplify Eq. (28) will result in.

$$J^T B\dot{X} - J^T B\dot{X}_d + J^T K(X - X_d) = -\tau_h - J^T F_g \tag{29}$$

$$J^T B\dot{X}_d = \tau_h + J^T F_g + J^T K(X - X_d) + J^T B\dot{X} \tag{30}$$

Substituting $\dot{X}_d = J\dot{q}_d$ [23] into Eq. (30) to obtain the velocity of the endpoint, gives.

$$J^T BJ\dot{q}_d = \tau_h + J^T F_g + J^T K(X - X_d) + J^T B\dot{X} \tag{31}$$

Eq. (31) is simplified to derive the equation for the motion intention estimator

$$\dot{q}_d = \frac{\tau_h + J^T F_g + J^T[B\dot{X} + K(X - X_d)]}{B\, J^T J} \tag{32}$$

where,
τ_h is the interaction torque from the therapist
J is the Jacobian matrix

$$J = \begin{bmatrix} -l\sin q \\ l\cos q \\ l \end{bmatrix} \tag{33}$$

According to the equation, each joint's intended velocity will change throughout active training sessions as the interaction torques from the associated joint change. Contact torques, departure from the endpoint's reference trajectory, and the damping impedance coefficient B, all have an impact on the rate of current changes. The desired velocity of each joint modifies when the endpoint position deviates from the prescript trajectory, bringing the subject back to the reference trajectory, indicating $X_d \neq X$. The adjustment range is determined by the stiffness and damping impedance coefficients $K$and B [24]. The interaction controller outputs the required joint velocity $\dot{q}_d$, which the SMC-FAT adaptive controller will use. Fig.3 shows the block diagram for the motion intention controller.

3.3.SMC-FAT-based Adaptive Controller

The motion intention estimator is integrated into the SMC-FAT based adaptive controller to get the desired motion and cater to the uncertainties in the lumped robot and human arm plant. The SMC-FAT controller equation used in the proposed control law for the feedback loop is written as [25].

$$X_a = [q \quad \dot{q} \quad \ddot{q}]^T \tag{34}$$

$$X_{da} = [q_d \quad \dot{q}_d \quad \ddot{q}_d]^T \tag{35}$$

$$U_s(t) = U_{eq} + U_{PI} + U_a \tag{36}$$

https://doi.org/10.31436/iiumej.v24i1.2604

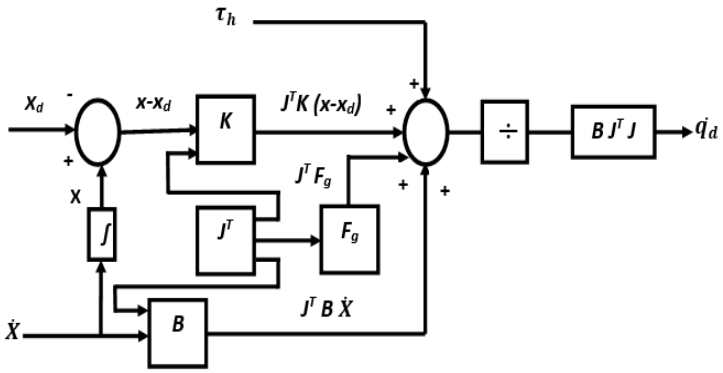

Fig. 3. Block diagram of motion intention estimator

The measured (actual trajectory) and desired (desired trajectory) state variables can be represented by vectors X_a and X_{da} respectively.
where, U_s , U_{eq} , U_{PI} and U_a terms of the proposed controller are described below. The U_s is the control signal supplied to the plant. The equivalent control term U_{eq} is considered for the approximately known nominal system [25].

$$U_{eq} = \bar{B_B}^{-1}(\dot{X}_r - \bar{A_B}X_a) \tag{37}$$

where, $\bar{A_B}$ and $\bar{B_B}$ represent the nominal matrices of A_B and $B_B$respectively.
X_a is the actual trajectory
$\dot{X}_r$ is the reference acceleration and it is denoted by the term $\dot{X}_{da} - \frac{{\lambda_2}^2 e}{2\lambda_1}$

The second term of the control strategy U_{PI} is a sort of PI (Proportional Integral) controller that is required to increase closed-loop stability and transient performance.

$$U_{PI} = -\bar{B_B}^{-1}K_1 S(t) = -\bar{B_B}^{-1}K_1(2\lambda_1 e + {\lambda_2}^2 \int e dt) \tag{38}$$

where, K_1 is a positive definite constant and $S(t)$ is the sliding surface of the controller
λ_1 and λ_2 are $n \times n$ diagonal positive definite matrix
$e = X_a - X_{da}$ is the tracking error vector
The term U_a is the term used to describe the process of removing approximation errors.

$$U_a = -\bar{B_B}^{-1}K_0\hat{\alpha}_0[sgn(S(t))] \tag{39}$$

where, K_0 is a constant, $\hat{\alpha}_0$is the estimation of α_0, and the upper bound of the uncertainties.

Substituting Eq. (37), Eq. (38), and Eq. (39), into Eq. (36), as shown below.

$$U_s(t) = \bar{B_B}^{-1}(\dot{X}_r - \bar{A}X_a - K_1 S - K_0\hat{\alpha}_0[sgn(S(t))]) \tag{40}$$

A detailed explanation of the derivation and stability proof of the controller can be found in [25].

3.4.Simulation Results

The simulation was carried out using different values of the constant and sinusoidal waveform for the torque exerted by the therapist. This research focuses on a 1 DOF upper limb rehabilitation arm, therefore only one motor is used in the verification experiment. The motion intention estimator based on impedance control as in Section 3.2, is adopted for the motion intention controller. The impedance parameters of the motion intention controller are set as $K = 0.34$ N/m and $B = 50Ns$/m. The extra gravity compensated force is set at $F_g = [0; 0; 0]$

N initially. The SMC-FAT controller parameters are set as $\lambda_1 = 50$, $\lambda_2 = 1$, $K_0 = 1$ and $K_1 = 337$.

Fig. 4 and 5 shows the tracking performance of the motion intention controller using a constant torque and sinusoidal waveform respectively. The range of the constant torque was calculated using the formula in Eq. (41) and the sinusoidal formula to represent the torque from the therapist is shown in Eq. (42).

$$\tau_h = F \times r \tag{41}$$

$$\tau_h = \mathrm{A}\sin(t) + \emptyset \tag{42}$$

In Fig.4 the red line shows the actual angular velocity and the dash blue line represents the desired angular velocity. It can be seen that the actual angular velocity follows the desired angular velocity that is calculated using the therapist's motion intention estimation based on his/her input torque τ_h. This result shows that the proposed control strategy has successfully calculated the therapist's motion intention and the robot follows the prescribed velocity trajectory under the SMC-FAT based adaptive controller.

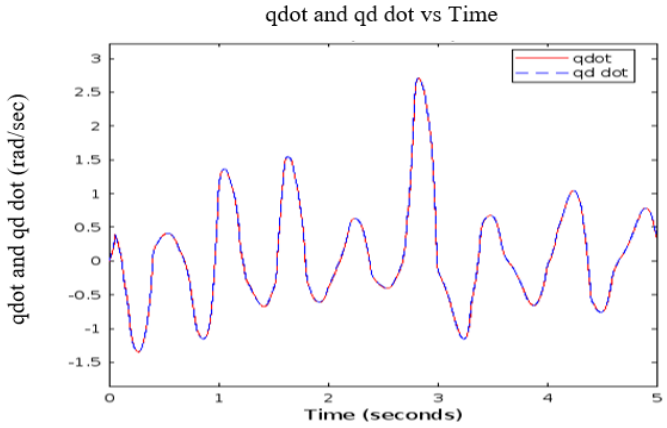

Fig.4. Tracking performance of the proposed control strategy at constant τ_h

Fig. 5 shows the tracking performance of the motion intention estimator using the sinusoidal equation, $\tau_h = \sin(2) + 11.76\ Nm$ to represent variation in the torque exerted by the therapist. It can be seen in Fig. 5 below that the actual angular velocity follows the desired angular velocity resulting from the motion intention estimator, under the proposed control law strategy.

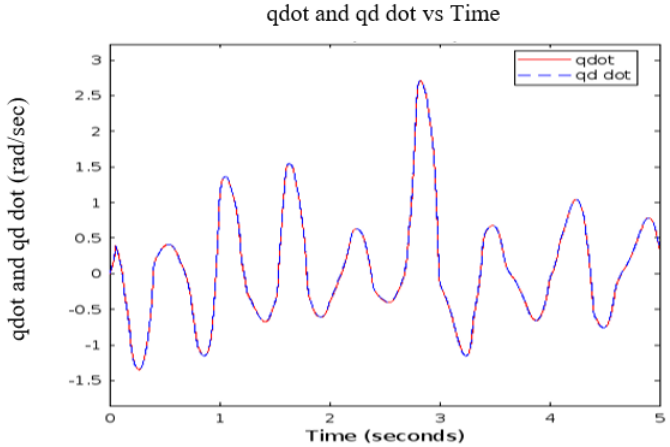

Fig.5. Tracking performance of the proposed control strategy at sinusoidal torque

From the simulation results, it can be observed that the proposed controller is effective. The motion intention estimator produces the desired velocity based on the therapist's torque. This

https://doi.org/10.31436/iiumej.v24i1.2604

value was fed into the SMC-FAT controller and the robot follows the desired trajectory precisely. The average percentage error at sample time of 5 seconds is 0.002rad/sec and 0.005rad/sec for constant and sinusoidal therapist's torque respectively.

4. SIMULATION RESULTS AND EXPERIMENTAL ANALYSIS

The simulation of the motion controller has been conducted using MATLAB Simulink for different inputs of torque and the experimental analysis is done with the aid of LabVIEW from National Instruments (NI).

4.1.Experimental Results

The experimental setup consists of 1 DOF robot arm and computer installed with LabVIEW to control the robot arm with the proposed motion intention estimator. LabVIEW is used to test and analyze the proposed motion intention controller on the robot arm. The National Instruments Data Acquisition (NI DAQmx) driver has been installed along with LabVIEW into the computer to aid the communication between the robot and the computer. The computer that is installed with LabVIEW is connected to the robot using the NI USB-6211 DAQ. The schematic diagram of the control strategy and motion intention estimator has been built in LabVIEW and run to check for errors. After the schematic has been verified, the robot is powered on, and the LabVIEW programming is launched. The robot motor torque, robot position, actual angular velocity, and desired angular velocity are displayed on the interface of the LabVIEW on the computer.

The motion intention controller impedance parameters are set as $K = 0.34$ N/m and $B = 50Ns$/m. The gravity force is set at $F_g = [0; 0; 0]$ N at first. The SMC-FAT controller parameters are set as $\lambda_1 = 50$, $\lambda_2 = 1$, $K_0 = 1$ and $K_1 = 337$. The experimental result of the robot's joint angular velocity is shown in Fig. 6.

Fig. 6 shows the desired angular velocity trajectory based on the therapist's motion intention estimation, $\dot{q}_d$ and the actual angular velocity $\dot{q}$, under the control of the SMC-FAT controller.

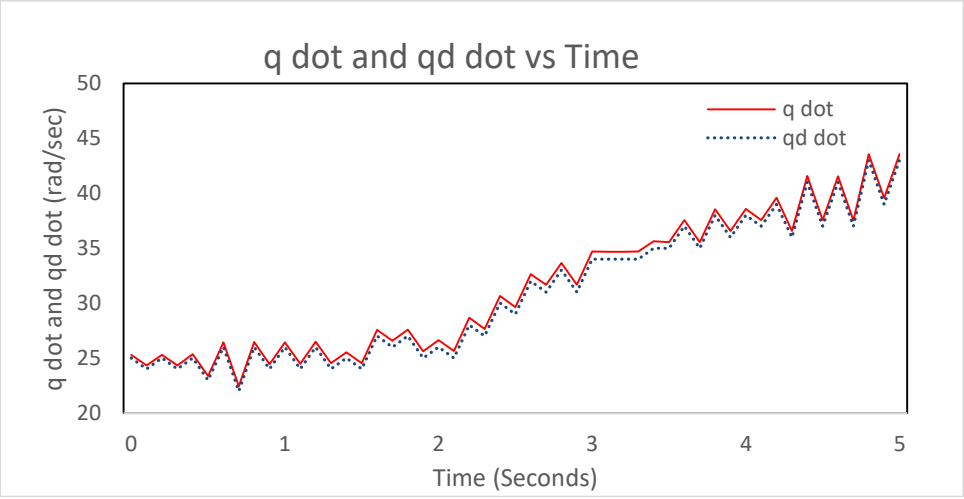

Fig.6. Experimental result of actual angular velocity and desired angular velocity against time using human torque

Fig.7 shows the corresponding therapist's torque during the experiment. The result shows that the controller produces the estimated motion intention based on the torque exerted by the therapist and drives the robot to track the resulting desired trajectory.

https://doi.org/10.31436/iiumej.v24i1.2604

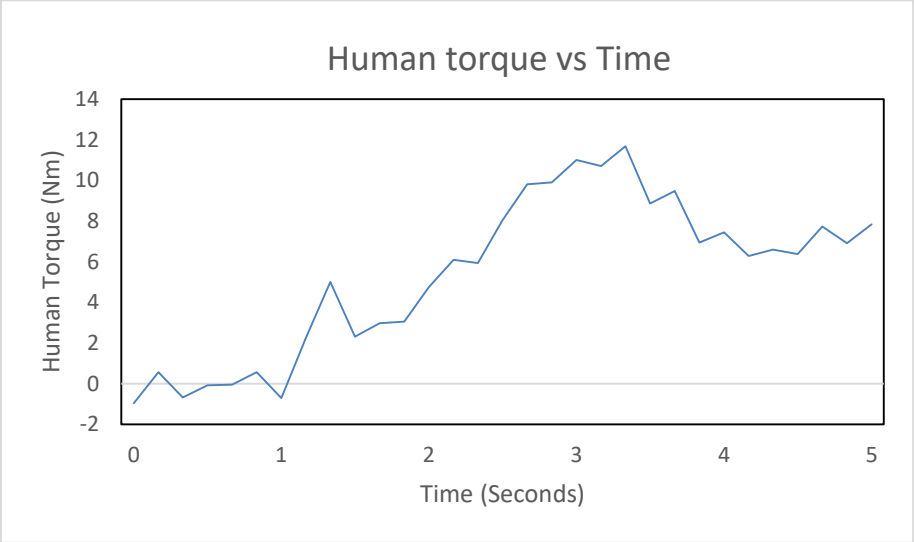

Fig.7. Therapist's torque input in hardware experimental test

From the simulation results and hardware experiment, it can be observed that the proposed controller is effective in generating the desired angular velocity, $\dot{q}_d$ based on the motion intention of the therapist and controlling the upper limb rehabilitation robot to follow the desired trajectory. The results verify that the proposed control strategy is successful. The therapist's motion intention can be predicted for the upper limb rehabilitation robot based on the torque exerted by the therapist under the proposed technique. The SMC-FAT - based adaptive controller integrated into the motion intention estimator can overcome the uncertainties in the robot and human arm parameters. The maximum error is 0.02rad for the hardware experiments.

5. CONCLUSION

A new control method has been formulated for therapists' motion intention estimation in a power assist upper limb rehabilitation robot based on impedance controller. The controller uses the therapist's interaction torque to estimate his/her motion intention and produces the desired angular velocity for the feedback controller. The SMC-FAT adaptive controller implemented in the feedback loop overcomes the uncertainties, in the lumped rehabilitation robot and human arm plant. Integrating the formulated motion intention estimator and SMC-FAT Adaptive control yields high tracking accuracy with the therapist's motion intention. The simulation results and hardware experiment validated that the proposed control strategy is successful in producing the motion intention estimation and accurate trajectory tracking with a maximum error of 0.005 rad/sec and 0.02 rad/sec respectively. In future work, the integrated motion intention controller and SMC-FAT controller can be used for a higher DOF of the upper limb rehabilitation robot arm system. Other types of uncertainties can also be considered in future studies.

ACKNOWLEDGEMENT

The authors would like to thank International Islamic University Malaysia (IIUM) for sponsoring this study under grant number P-RIGS 18-019-0019.

REFERENCES

[1] Eiammanussakul, T., and Sangveraphunsiri, V. (2018). A lower limb rehabilitation robot in sitting position with a review of training activities. Journal of Healthcare Engineering, 2018, 1–18.
[2] Bogue, R. (2018). Rehabilitation robots. Industrial Robot, 45(3), 301–306.
[3] Alrabghi, L., Alnemari,R., Aloteebi, R., Alshammari, H., Ayyad, M., Al Ibrahim,M., Alotayfi, M., Bugshan, T., Alfaifi, A., and Aljuwayd, H. (2018). Stroke types and management. International Journal Of Community Medicine And Public Health, 5(9), 3715.
[4] Tang, Z., Zhang, K., Sun, S., Gao, Z., Zhang, L., and Yang, Z. (2014). An upper-limb power-assist exoskeleton using proportional myoelectric control. Sensors (Switzerland), 14(4), 6677–6694.
[5] Kadota, K., Akai, M., Kawashima, K., and Kagawa, T. (2009). Development of power-assist robot arm using pneumatic rubber muscles with a balloon sensor. Proceedings - IEEE International Workshop on Robot and Human Interactive Communication, 546–551.
[6] Liu, Z., and Hao, J. (2019). Intention Recognition in Physical Human-Robot Interaction Based on Radial Basis Function Neural Network. Journal of Robotics, 2019, 1–8.
[7] Lee, J., Kim, M., Ko, H., and Kim, K. (2014). A control method of power-assisted robot for upper limb considering intention-based motion by using sEMG signal. 2014 11th International Conference on Ubiquitous Robots and Ambient Intelligence, URAI 2014, 385–390.
[8] Huang, J., Huo, W., Xu, W., Mohammed, S., and Amirat, Y. (2015). Control of Upper-Limb Power-Assist Exoskeleton Using a Human-Robot Interface Based on Motion Intention Recognition. IEEE Transactions on Automation Science and Engineering, 12(4), 1257–1270.
[9] Li, M., Deng, J., Zha, F., Qiu, S., and Wang, X. (2018). Motion Intention Estimation for Active Power-Assist Lower Limb Exoskeleton Robot (APAL). Preprints, 1–20.
[10] Chathuramali, K. G. M., and Kiguchi, K. (2020). Real-time detection of the interaction between an upper-limb power-assist robot user and another person for perception-assist. Cognitive Systems Research, 61, 53–63.
[11] Struk, S., Correia, N., Guenane, Y., Revol, M., and Cristofari, S. (2018). Full-thickness skin grafts for lower leg defects coverage: Interest of postoperative immobilization. Annales de Chirurgie Plastique Esthetique, 63(3), 229–233.
[12] Wang, X., Li, X., and Wang, J. (2015). Modeling and identification of the human-exoskeleton interaction dynamics for upper limb rehabilitation. Lecture Notes in Electrical Engineering, 338, 51–60.
[13] Lee, J., Kim, M., and Kim, K. (2017). A control scheme to minimize muscle energy for power assistant robotic systems under unknown external perturbation. IEEE Transactions on Neural Systems and Rehabilitation Engineering, 25(12), 2313–2327.
[14] Nomura, S., Takahashi, Y., Sahashi, K., Murai, S., Taniai, Y., and Naniwa, T. (2019). Power assist control based on human motion estimation using motion sensors for powered exoskeleton without binding legs. Applied Sciences (Switzerland), 9(1), 14–16.
[15] Zhuang, Y., Yao, S., Ma, C., and Song, R. (2019). Admittance Control Based on EMG-Driven Musculoskeletal Model Improves the Human-Robot Synchronization. IEEE Transactions on Industrial Informatics, 15(2), 1211–1218.
[16] Wang, W., Zhang, J., Kong, D., Su, S., Yuan, X., & Zhao, C. (2022). Research on control method of upper limb exoskeleton based on mixed perception model. Robotica, 1–17.
[17] Wang, W., Qin, L., Yuan, X., Ming, X., Sun, T., and Liu, Y. (2019). Bionic control of exoskeleton robot based on motion intention for rehabilitation training. Advanced Robotics, 33(12), 590–601.
[18] Yang, C., Chen, C., He, W., Cui, R., and Li, Z. (2019). Robot Learning System Based on Adaptive Neural Control and Dynamic Movement Primitives. IEEE Transactions on Neural Networks and Learning Systems, 30(3), 777–787.
[19] Shanta, M. N. T., and Azlan, N. Z. (2015). Function Approximation Technique based Sliding Mode Controller Adaptive Control of Robotic Arm with Time-Varying Uncertainties. Procedia Computer Science, 76, 87–94.

[20] Osman, J. (1990). Modeling and control of robot manipulators. Dissertation, City University London.https://openaccess.city.ac.uk/id/eprint/7758/1/Decentralized_and_hierarchical_control_of_robot_manipulators.pdf
[21] Adeola-Bello, Z., & Azlan, N. (2022). Power Assist Rehabilitation Robot and Motion Intention Estimation. International Journal of Robotics and Control Systems, 2(2), 297-316.
[22] Song, P., Yu, Y., and Zhang, X. (2019). A Tutorial Survey and Comparison of Impedance Control on Robotic Manipulation. Robotica, 37(5), 801-836.
[23] Xing, L., Wang, X., and Wang, J. (2017). A motion intention-based upper limb rehabilitation training system to stimulate motor nerve through virtual reality. International Journal of Advanced Robotic Systems, 14(6), 1–8.
[24] Topini, A., Sansom, W., Secciani, N., Bartalucci, L., Ridolfi, A., andAllotta, B. (2022). Variable Admittance Control of a Hand Exoskeleton for Virtual Reality-Based Rehabilitation Tasks. Frontiers in neurorobotics, 15, 789743.
[25] Shanta, M. N. T., and Azlan, N. Z. (2016). Adaptive sliding mode control with radial basis function neural network for time dependent disturbances and uncertainties. ARPN Journal of Engineering and Applied Sciences, 11(6), 4123–4129.